

Journal of Materials Chemistry C

Accepted Manuscript



This is an *Accepted Manuscript*, which has been through the Royal Society of Chemistry peer review process and has been accepted for publication.

Accepted Manuscripts are published online shortly after acceptance, before technical editing, formatting and proof reading. Using this free service, authors can make their results available to the community, in citable form, before we publish the edited article. We will replace this *Accepted Manuscript* with the edited and formatted *Advance Article* as soon as it is available.

You can find more information about *Accepted Manuscripts* in the [Information for Authors](#).

Please note that technical editing may introduce minor changes to the text and/or graphics, which may alter content. The journal's standard [Terms & Conditions](#) and the [Ethical guidelines](#) still apply. In no event shall the Royal Society of Chemistry be held responsible for any errors or omissions in this *Accepted Manuscript* or any consequences arising from the use of any information it contains.



Journal Name

COMMUNICATION

Multi-Carbazole Encapsulation as A Simple Strategy for Constructing Solution-Processed, Non-Doped Thermally Activated Delayed Fluorescence Emitters

Received 00th January 20xx,
Accepted 00th January 20xx

DOI: 10.1039/x0xx00000x

www.rsc.org/

Jiajia Luo,† Shaolong Gong,† Yu Gu, Tianheng Chen, Yifan Li, Cheng Zhong, Guohua Xie and Chuluo Yang*

Two TADF emitters are developed by introducing carbazole dendrons into the multi-positions of a blue TADF emissive core. By utilizing these TADF emitters as the non-doped solution-processed emissive layers, a greenish-blue OLED achieves a peak EQE of 12.2%, which is among the highest value for non-doped solution-processed fluorescent OLEDs.

Purely organic thermally activated delayed fluorescent (TADF) emitters have been explored as the most promising third generation of emissive materials for organic light-emitting diodes (OLEDs),^[1] following the first generation of conventional fluorescent materials^[2] and the second generation of phosphorescent heavy-metal complexes.^[3] Their merit of up-converting non-radiative triplet excitons into radiative singlet excitons allows the harvest of both singlet and triplet excitons, and thereby approach an internal quantum efficiency of 100% theoretically.^[4] Up to now, Adachi et al. has developed numerous small-molecule TADF emitters with peak external quantum efficiencies (EQEs) comparable with phosphorescent OLEDs, which are suitable for vacuum deposition process.^[5] However, the large-scale deployment of OLEDs requires solution process to make fabrication process simple, cost-effective and controllable.^[6] Therefore, the further focus of TADF research should be on developing solution-processed TADF emitters.

Very recently, several small-molecule TADF emitters have been employed in the solution-processed OLEDs and achieved relatively high EQEs.^[7,8] For example, Kaji et al. demonstrated a maximum EQE of 18.6% by utilizing a bluish-green TADF emitter;^[7] Su et al. reported a maximum EQE of 17.5% by using

a green TADF emitter.^[8c] Although promising EQEs have been achieved for solution-processed TADF emitters, all of the TADF emitters in the devices have to be doped into some host materials.^[7-9] To further reduce processing complexity and module costs, the development of non-doped solution-processable TADF emitters is of important significance.

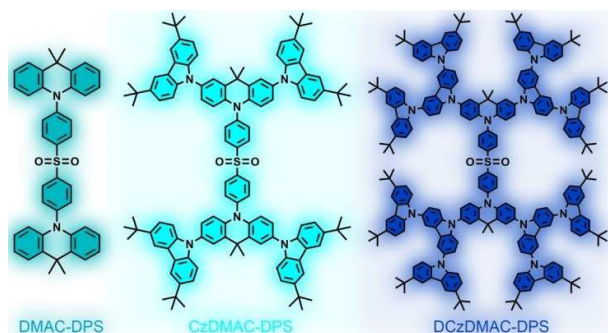
Carbazole unit is considered as the widely used building block for functional materials in OLEDs because of its good hole-transporting ability, amorphous film-forming property, high triplet energy and good thermal stability.^[10] Previous studies on carbazole derivatives have uncovered the great potential of carbazole unit for constructing non-doped emitters.^[11] Herein, we present a multi-carbazole encapsulation strategy on the design of solution-processed and non-doped TADF emitters by introducing carbazole dendrons into the multi-positions of a TADF emissive core, 10,10'-(sulfonylbis(4,1-phenylene))bis(9,9-dimethyl-9,10-dihydroacridine) (DMAC-DPS), which has been proven to be an excellent blue TADF emitter peaking at 470 nm in neat film with a high photoluminescence quantum yield (PLQY) of 0.88 (Scheme 1).^[12] This strategy could not only improve hole injection and transport ability, but also minimize concentration quenching approach, consequently reduce efficiency quenching in OLEDs. The resulting multi-carbazole encapsulated emitters exhibit blue emission with obvious TADF feature and high PLQY. The double-layer blue device based on these non-doped emitters achieves a peak EQE of 12.2% with the CIE coordinates of (0.22, 0.44). This value is among the highest EQEs for non-doped and solution-processed fluorescent OLEDs.

Multi-carbazole encapsulated compounds were obtained through a two-step synthesis in moderate yields (Scheme S1). Iodization of DMAC-DPS with *N*-iodosuccinimide (NIS) produced the key intermediate, 10,10'-(sulfonylbis(4,1-phenylene))bis(2,7-diiodo-9,9-dimethyl-9,10-dihydroacridine) (4I-DMAC-DPS), then it was subsequently coupled with 3,6-di-*tert*-butyl-9*H*-carbazole (R1-H) or 3,3'',6,6''-tetra-*tert*-butyl-9'*H*-9,3':6',9''-tercarbazole (R2-H) through Cu-catalyzed C-N cross-coupling reaction to afford the target

* Hubei Collaborative Innovation Center for Advanced Organic Chemical Materials, Hubei Key Lab on Organic and Polymeric Optoelectronic Materials, Department of Chemistry, Wuhan University, Wuhan, 430072, People's Republic of China. E-mail: clyang@whu.edu.cn

† These authors contributed equally to this work.

‡ Electronic Supplementary Information (ESI) available: Experimental section, synthetic scheme, NMR spectra, MALDI-TOF and elemental analyses of TADF materials; TGA and DSC curves, density functional theory calculations, atomic force microscope and time-resolved transient fluorescence spectra data for TADF materials. See DOI: 10.1039/c000000x/



Scheme 1. Molecular structures of TADF materials.

compounds of CzDMAC-DPS and DCzDMAC-DPS, respectively. These compounds were identified by ^1H NMR and ^{13}C NMR spectroscopy, elemental analysis and MALDI-TOF mass spectrometry. CzDMAC-DPS and DCzDMAC-DPS exhibit good solubility in common organic solvents, such as THF, chloroform, toluene and chlorobenzene. These compounds decompose at 459 and 479 $^\circ\text{C}$ with a 5% weight loss, respectively, and exhibit ultrahigh glass transition temperatures of 272 and 274 $^\circ\text{C}$, respectively (Fig. S1 and Table S1). Such good solubility and excellent thermal stability of these compounds guarantee homogeneous and stable amorphous thin films *via* a solution process, which is indispensable for solution-processed OLEDs. The electrochemical cyclic voltammetry (CV) curves of CzDMAC-DPS and DCzDMAC-DPS exhibit two quasi-reversible, one-electron oxidation processes (Fig. S2), which can be assigned to the oxidation of DMAC and carbazole dendrons, respectively.^[10,11] The highest occupied molecular orbital (HOMO) levels of CzDMAC-DPS and DCzDMAC-DPS are estimated to be -5.24 and -5.18 eV, respectively, which match well to the HOMO level (-5.2 eV) of PEDOT:PSS. Their lowest unoccupied molecular orbital (LUMO) levels are estimated to be -2.31 eV for CzDMAC-DPS and -2.09 eV for DCzDMAC-DPS by using the optical bandgaps and HOMO levels. Their HOMO/LUMO levels are basically consistent with the calculated HOMO/LUMO levels (Table 1) from the density functional theory (DFT) calculation for these emitters.

Fig. 1 depicts the absorption, PL and phosphorescence spectra of CzDMAC-DPS and DCzDMAC-DPS in neat films. Both compounds display two types of absorption bands simultaneously: the absorption bands at 240 and 299 nm assigned to the π - π^* transition of carbazole dendrons,^[13] the absorption bands in the range of 320-

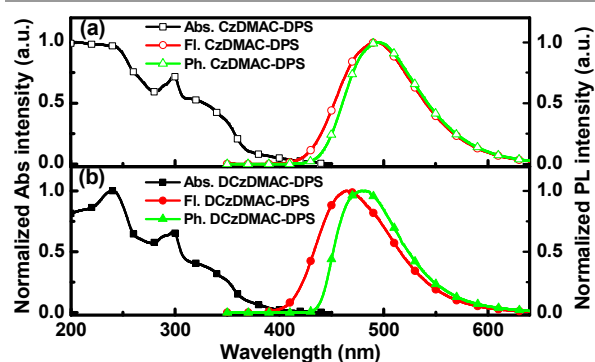


Fig. 1 The absorption, photoluminescence and phosphorescence spectra of CzDMAC-DPS (a) and DCzDMAC-DPS (b) in neat films.

Table 1. The theoretical data of TADF materials obtained from the DFT calculation.

compound	HOMO/LUMO (eV)	F^a	S_1 (eV)	T_1 (eV)	ΔE_{ST} (eV)
DMAC-DPS	-5.92/-2.92	0.0001	2.76	2.75	0.01
CzDMAC-DPS	-4.96/-2.02	0.0003	2.52	2.51	0.01
DCzDMAC-DPS	-5.20/-2.36	0.0005	2.58	2.50	0.08

^a oscillator strength.

370 nm assigned to the charge-transfer (CT) transition from the 9,9-dimethyl-9,10-dihydroacridine (DMAC) and the carbazole dendrons to the diphenyl sulfoxide (DPS) unit.^[14] With the increasing generation of carbazole dendrons, the absorption intensity of CT bands is reduced (Table S1), which suggests that the CT transition state get weak.^[15] As shown in Fig. 1, the neat films of CzDMAC-DPS and DCzDMAC-DPS exhibit broad emission bands with the emission peaks at 492 and 464 nm, respectively. With respect to the emission peak of 470 nm for the parent compound of DMAC-DPS, the emission peak of CzDMAC-DPS (492 nm) shows a significant red-shift, while the emission peak of DCzDMAC-DPS (464 nm) exhibits a slight blue-shift. This phenomenon can be elucidated from the degree of CT for these emitters as shown in DFT calculations (Fig. S3). The DFT results revealed that DMAC-DPS possesses a well-separated HOMO and LUMO distribution that localize on DMAC and DPS units, respectively (Fig. S3), which is consistent with the previously reported result. The LUMOs of CzDMAC-DPS and DCzDMAC-DPS are still located on DPS unit, the same as DMAC-DPS. The HOMO of CzDMAC-DPS delocalizes over its DMAC and carbazole dendrons, and thereby results in a strong CT feature that induces a red-shift of emission peak. Differently, the HOMO of DCzDMAC-DPS mainly distributes over the outer carbazole dendrons, instead of DMAC, which consequently makes the CT nature weak and a blue-shift of emission peak with respect to DMAC-DPS and CzDMAC-DPS. The same trend can also be observed for their PL spectra in toluene (Fig. S4). The singlet and triplet state energy are estimated from the onsets of the fluorescence and phosphorescence spectra, respectively, and the energy gaps between the singlet and triplet state energy (ΔE_{ST}) are 0.09 eV for CzDMAC-DPS and 0.20 eV for DCzDMAC-DPS (Table S1),

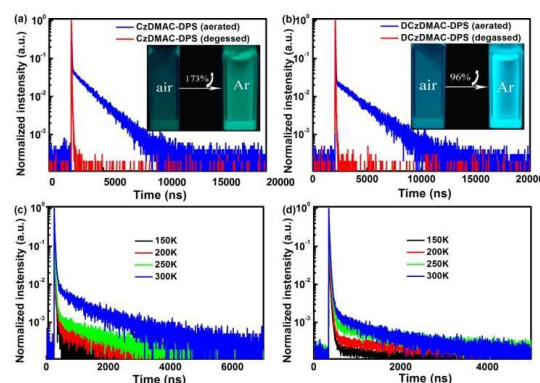


Fig. 2 The transient photoluminescence decay spectra of CzDMAC-DPS (a) and DCzDMAC-DPS (b) in toluene. Insets: photographs showing the enhancement of the emitting intensity for CzDMAC-DPS (173%) and DCzDMAC-DPS (96%) in toluene when changing from the aerated to degassed condition. The transient photoluminescence decay spectra of CzDMAC-DPS (c) and DCzDMAC-DPS (d) in film at various temperatures.

which coincide well with the ΔE_{ST} s obtained from time-dependent DFT calculation for these emitters. Such small ΔE_{ST} s implicates that their triplet states could be easily utilized by reverse intersystem crossing process based on $T_1 \rightarrow S_1$.^[16]

To further understand the emissive nature of these emitters, their transient PL characteristics both in toluene and in neat film were measured. As shown in Fig. 2a and 2b, CzDMAC-DPS and DCzDMAC-DPS exhibit single exponential decay in toluene with the short lifetimes of 16.4 and 16.1 ns, respectively. In contrast, they display a second-order exponential decay with prompt (28.5 ns for CzDMAC-DPS and 25.8 ns for DCzDMAC-DPS) and delayed (1.54 μ s for CzDMAC-DPS and 1.91 μ s for DCzDMAC-DPS) components in toluene under oxygen-free condition. This implies that the triplet states of the emitters are involved in the emissive process. Moreover, the temperature dependence of the transient PL decay for CzDMAC-DPS and DCzDMAC-DPS neat films reveals typical TADF feature, i.e., the delayed component gradually increases when raising the temperature from 150 to 300 K (see Fig. 2c and 2d).^[1b,16b] The total PLQYs of CzDMAC-DPS and DCzDMAC-DPS in neat film were measured to be 0.68 and 0.48 under Ar condition, respectively, which indicates that CzDMAC-DPS and DCzDMAC-DPS could be used as potentially good emitters in OLEDs.

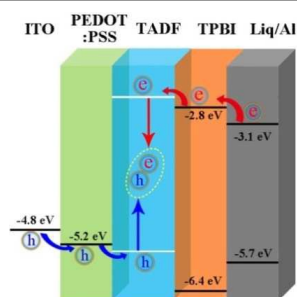


Fig. 3 Schematic and energy level diagrams for the double-layer solution-processed OLEDs.

In view of the above-mentioned excellent properties of CzDMAC-DPS and DCzDMAC-DPS, their neat films are favorable for using as the emitting layer in the solution-processed OLEDs. The double-layer solution-processed OLEDs with an architecture of indium tin oxide (ITO)/PEDOT:PSS (40 nm)/EML (40 nm)/TPBI (40 nm)/Liq (1.6 nm)/Al (100 nm) were fabricated (Fig. 3), where poly(3,4-ethylenedioxythiophene):poly(styrenesulfonic acid) (PEDOT:PSS) and 8-hydroxyquinolinolato-lithium (Liq) serve as the hole- and electron-injection layer, respectively; 1,3,5-tris(*N*-phenylbenzimidazole-2-yl)benzene (TPBI) acts as the electron-transporting layer,^[1a] CzDMAC-DPS and DCzDMAC-DPS are employed as the emissive layers, respectively. For comparison, we also fabricated the control device A using the emissive core, DMAC-DPS, as the EML. The devices based on DMAC-DPS, CzDMAC-DPS and DCzDMAC-DPS are denoted as device A, B, and C, respectively.

Fig. 4 presents the EL spectra, current density-voltage-luminance characteristics, and power efficiency and external quantum efficiency versus current density for the devices. The key EL parameters are summarized in Table 2. The devices A and C exhibit true blue emission with the similar CIE coordinates of (0.18, 0.31) and (0.18, 0.27), respectively; while the device B based on CzDMAC-

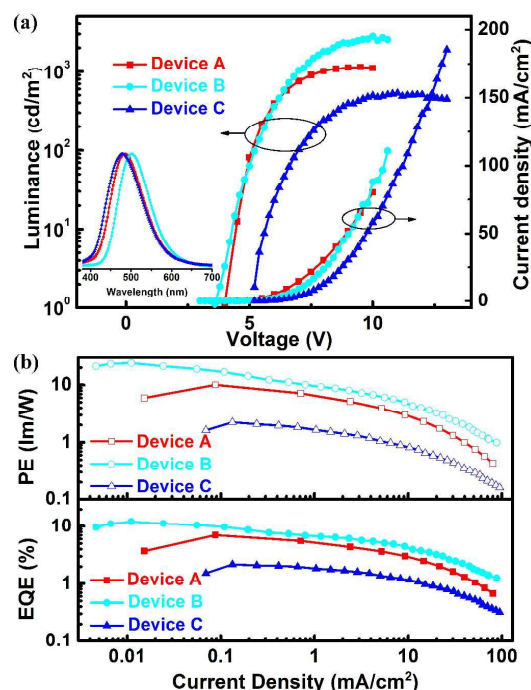


Fig. 4 (a) Current density-voltage-luminance curves of the devices. Inset: Electroluminescence spectra of the devices. Inset: EL spectra of devices A-C at the driving voltage of 10 V. (b) Power efficiency and External quantum efficiency versus current density for the devices.

DPS displays greenish-blue emission with the CIE coordinates of (0.22, 0.44). All the EL spectra are consistent with the corresponding PL spectra of their neat films. Device C with DCzDMAC-DPS as EML displays significantly higher turn-on voltage of 5.2 V than those of devices based on DMAC-DPS (4.0 V) and CzDMAC-DPS (3.6 V). This can be attributed to the high-lying LUMO level of -2.09 eV for DCzDMAC-DPS,^[17] which leads to a large electron injection barrier of about 0.7 eV. Device C achieves a maximum current efficiency (CE_{max}) of 3.8 cd/A, a maximum power efficiency (PE_{max}) of 2.0 lm/W, and a maximum EQE of 2.2%, which are lower than those of the control device A based on DMAC-DPS (11.4 cd/A, 10.1 lm/W, 7.0%). This can be ascribed to the low PLQY (48.2%) and the large electron injection barrier for DCzDMAC-DPS. The best device performance is achieved for CzDMAC-DPS-based device B, with the CE_{max} of 30.6 cd/A, the PE_{max} of 24.0 lm/W and the EQE_{max} of 12.2%. This device performance is among the highest values for non-doped solution-processed fluorescent OLEDs.

Why device B based on CzDMAC-DPS achieves the outstanding performance? We further investigate its morphology of spin-coated neat films by atomic force microscope (AFM). As shown in Fig. S5, CzDMAC-DPS shows the root mean square (RMS) of 0.282 nm that is relatively lower than that of the pristine DMAC-DPS (0.433 nm). The desirable morphology should be attributed to the introduction of carbazole-dendrons. In a word, the high efficiency of CzDMAC-DPS-based device B can be explained by its superiority: the small ΔE_{ST} value to ensure the effective RISC process based on $T_1 \rightarrow S_1$; the high PLQY to provide an intrinsically high-efficiency emission; good solution processability and film-forming ability to render smooth surface morphology and reduce non-radiative process in the quenching center.

Table 2. The key EL data for devices A-C.

device	EML	V_{on} ^a (V)	$V_{max}/CE_{max}/PE_{max}/EQE_{max}$ ^b (V/cd A ⁻¹ /lm W ⁻¹ /%)	$V_{100}/CE_{100}/PE_{100}/EQE_{100}$ ^c (V/cd A ⁻¹ /lm W ⁻¹ /%)	$V_{1000}/CE_{1000}/PE_{1000}/EQE_{1000}$ ^d (V/cd A ⁻¹ /lm W ⁻¹ /%)	CIE (x, y) ^e
A	DMAC-DPS	4.0	4.5/11.4/10.1/7.0	5.5/9.0/5.2/4.4	8.0/3.4/1.3/1.6	(0.18, 0.31)
B	CzDMAC-DPS	3.6	4.0/30.6/24.0/12.2	5.4/17.4/10.1/6.9	7.0/11.3/5.1/4.5	(0.22, 0.44)
C	DCzDMAC-DPS	5.2	5.4/3.8/2.0/2.2	7.0/2.7/1.2/1.5	NA	(0.18, 0.27)

^a The driving voltage at 1 cd/m². ^b The driving voltage (V_{max}) for maximum CE, maximum current efficiency (CE_{max}), maximum power efficiency (PE_{max}) and maximum external quantum efficiency (EQE_{max}). ^c V, CE, PE, and EQE at 100 cd/m². ^d V, CE, PE, and EQE at 1000 cd/m². ^e The Commission Internationale de L'Éclairage coordinates.

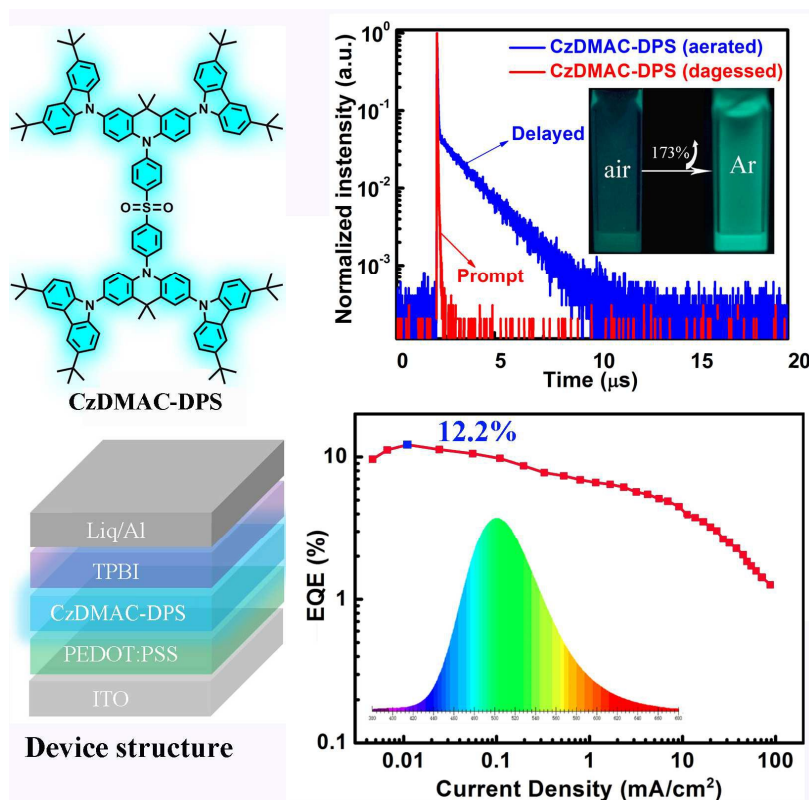
In summary, we develop two solution-processed blue TADF emitters by multi-carbazole encapsulation for a emissive core of DMAC-DPS. These compounds possess good solution processability, excellent thermal stability, obvious TADF feature and relatively high PLQYs. By employing these TADF emitters as the non-doped emissive layers in solution-processed OLEDs, a greenish-blue double-layer device achieves a peak EQE of 12.2% with the CIE coordinates of (0.22, 0.44), which is among the highest efficiency to date for non-doped solution-processed fluorescent OLEDs. This work provides a feasible strategy for developing solution-processable non-doped TADF emitters, and will pave a way towards practical application of solution-processable fluorescent OLEDs for large-area manufacturing.

Notes and references

We gratefully acknowledge financial support from the National Natural Science Foundation of China (Nos. 91433201, 51573141 and 51125013), the National Basic Research Program of China (973 Program 2015CB655002 and 2013CB834805), the Innovative Research Group of Hubei Province (No. 2015CFA014) and the Fundamental Research Funds for the Central Universities of China (2042015kf0033 and 2042015kf0007).

- (a) Y. Tao, K. Yuan, T. Chen, P. Xu, H. Li, R. Chen, C. Zheng, L. Zhang, W. Huang, *Adv. Mater.*, 2014, **26**, 7931; (b) H. Uoyama, K. Goushi, K. Shizu, H. Nomura, C. Adachi, *Nature*, 2012, **492**, 234; (c) S. Wang, X. Yan, Z. Cheng, H. Zhang, Y. Liu, Y. Wang, *Angew. Chem. Int. Ed.*, 2015, **54**, 13068.
- M. Zhu, C. Yang, *Chem. Soc. Rev.*, 2013, **42**, 4963.
- (a) T. Itoh, *Chem. Rev.*, 2012, **112**, 4541; (b) S. Gong, Y.-L. Chang, K. Wu, R. White, Z.-H. Lu, D. Song and C. Yang, *Chem. Mater.*, 2014, **26**, 1463.
- (a) F. B. Dias, K. N. Bourdakos, V. Jankus, K. C. Moss, K. T. Kamtekar, V. Bhalla, J. Santos, M. R. Bryce, A. P. Monkman, *Adv. Mater.*, 2013, **25**, 3707; (b) R. Ishimatsu, S. Matsunami, T. Kasahara, J. Mizuno, T. Edura, C. Adachi, K. Nakano, T. Imato, *Angew. Chem. Int. Ed.*, 2014, **53**, 6993; (c) G. Mehes, H. Nomura, Q. Zhang, T. Nakagawa, C. Adachi, *Angew. Chem. Int. Ed.*, 2012, **51**, 11311; (d) Q. Zhang, B. Li, S. Huang, H. Nomura, H. Tanaka, C. Adachi, *Nature Photon.*, 2014, **8**, 326.
- (a) S. Y. Lee, T. Yasuda, Y. S. Yang, Q. Zhang, C. Adachi, *Angew. Chem. Int. Ed.*, 2014, **53**, 6402; (b) K. Suzuki, S. Kubo, K. Shizu, T. Fukushima, A. Wakamiya, Y. Murata, C. Adachi, H. Kaji, *Angew. Chem. Int. Ed.*, 2015, **54**, 15231; (c) Q. Zhang, H. Kuwabara, W. J. Potscavage, Jr., S. Huang, Y. Hatae, T. Shibata, C. Adachi, *J. Am. Chem. Soc.*, 2014, **136**, 18070; (d) Q. Zhang, J. Li, K. Shizu, S. Huang, S. Hirata, H. Miyazaki, C. Adachi, *J. Am. Chem. Soc.*, 2012, **134**, 14706.
- (a) Y. J. Cho, K. S. Yook, J. Y. Lee, *Adv. Mater.*, 2014, **26**, 6642; (b) S. Shao, J. Ding, L. Wang, X. Jing, F. Wang, *J. Am. Chem. Soc.*, 2012, **134**, 20290; (c) J. Luo, G. Xie, S. Gong, T. Chen, C. Yang, *Chem. Commun.*, 2016, **52**, 2292.
- Y. Wada, K. Shizu, S. Kubo, K. Suzuki, H. Tanaka, C. Adachi, H. Kaji, *Appl. Phys. Lett.*, 2015, **107**, 183303.
- (a) K. Kawano, K. Nagayoshi, T. Yamaki, C. Adachi, *Org. Electron.*, 2014, **15**, 1695; (b) R. Komatsu, H. Sasabe, S. Inomata, Y. J. Pu, J. Kido, *Synth. Met.*, 2015, **202**, 165; (c) G. Xie, X. Li, D. Chen, Z. Wang, X. Cai, D. Chen, Y. Li, K. Liu, Y. Cao, S. Su, *Adv. Mater.*, 2016, **28**, 181.
- Y. J. Cho, B. D. Chin, S. K. Jeon, J. Y. Lee, *Adv. Funct. Mater.*, 2015, **25**, 6786.
- K. Albrecht, K. Matsuoka, K. Fujita, K. Yamamoto, *Angew. Chem. Int. Ed.*, 2015, **54**, 5677.
- (a) P. Moonsin, N. Prachumrak, S. Namuangruk, S. Jungstittiwong, T. Keawin, T. Sudyoasuk, V. Promarak, *Chem. Commun.*, 2013, **49**, 6388; (b) J. Ding, B. Wang, Z. Yue, B. Yao, Z. Xie, Y. Cheng, L. Wang, X. Jing, F. Wang, *Angew. Chem. Int. Ed.*, 2009, **48**, 6664; (c) D. Xia, B. Wang, B. Chen, S. Wang, B. Zhang, J. Ding, L. Wang, X. Jing, F. Wang, *Angew. Chem. Int. Ed.*, 2014, **53**, 1048.
- Q. Zhang, D. Tsang, H. Kuwabara, Y. Hatae, B. Li, T. Takahashi, S. Y. Lee, T. Yasuda, C. Adachi, *Adv. Mater.*, 2015, **27**, 2096.
- N. Prachumrak, S. Pojanasopa, S. Namuangruk, T. Kaewin, S. Jungstittiwong, T. Sudyoasuk, V. Promarak, *ACS Appl. Mater. Inter.*, 2013, **5**, 8694.
- Z. Xie, C. Chen, S. Xu, J. Li, Y. Zhang, S. Liu, J. Xu, Z. Chi, *Angew. Chem. Int. Ed.*, 2015, **54**, 7181.
- I. Hwang, U. Selig, S. S. Chen, P. E. Shaw, T. Brixner, P. L. Burn, G. D. Scholes, *J. Phys. Chem. A*, 2013, **117**, 6270.
- (a) A. E. Nikolaenko, M. Cass, F. Bourcet, D. Mohamad, M. Roberts, *Adv. Mater.*, 2015, **27**, 7236; (b) J. Zhang, D. Ding, Y. Wei, F. Han, H. Xu, W. Huang, *Adv. Mater.*, 2016, **28**, 479; (c) P. Rajamalli, N. Senthilkumar, P. Gandeepan, P.-Y. Huang, M.-J. Huang, C.-Z. Ren-Wu, C.-Y. Yang, M.-J. Chiu, L.-K. Chu, H.-W. Lin, C.-H. Cheng, *J. Am. Chem. Soc.*, 2016, **138**, 628.
- Y. J. Cho, K. S. Yook, J. Y. Lee, *Adv. Mater.*, 2014, **26**, 4050.

Graphic Abstract



Multi-carbazole encapsulation is demonstrated as a simple strategy for developing solution-processed TADF emitters. The resulting OLEDs achieve a recorded external quantum efficiency of 12.2% for non-doped solution-processed fluorescent OLEDs.